KINETIC FORMULAE FOR (D+D)μ AND (T+T)μ MUON-CATALYZED NUCLEAR SYNTHESIS

By M. Bubak*, V. M. Bystritsky and A. Guła**

Joint Institute for Nuclear Research, Dubna, USSR

(Received October 18, 1984; Final version received January 24, 1985)

General kinetic formulae taking into account an arbitrary number of μ-atomic and μ-molecular transitions in the chain leading to the muon-catalyzed nuclear synthesis in a D_2 or T_2 target with possible $Z > 1$ contaminations are derived. Application of the obtained formulae to the analysis of the experimental data is discussed.

PACS numbers: 25.70.Ij

1. Introduction

The advent of the exciting results from Los Alamos [1] indicating that one muon can catalyze about 80 acts of fusion $(d+t)\mu \rightarrow (^4He+n)\mu$ has stimulated discussions [2] about the fascinating prospects of employing "cold fusion" [3] in production of nuclear energy and, at the same time, has opened new questions concerning the physical picture of the muon-catalysis of the nuclear synthesis [4, 5]. For either reason the μ-atomic and μ-molecular processes leading to fusion in dtμ molecule deserve now a closer look. However, in experiments with the D_2–T_2 targets the presence of the competing channels leading to fusion in ddμ and ttμ molecules makes a more detailed study prohibitively complicated. Therefore, the parameters characterizing these two channels should be first determined in separate experiments with pure deuterium and pure tritium targets to provide the necessary input information for the analysis of the full (d+t)μ-fusion scheme.

The (d+d)μ-fusion has already been studied in several experiments [6–8]. More data would be desirable, however, to allow a better understanding of the processes involved and to resolve the discrepancies between the results of Refs. [7] and [8]. On the other hand, no data exist so far concerning the (t+t)μ-fusion. These should be available soon from the experiment planned in Dubna [9].

The chain of processes leading to the muon-catalyzed fusion in a target consisting

* On leave from the Institute of Computer Science, Academy of Mining and Metallurgy, Mickiewicza 30, 30-059 Kraków, Poland.

** On leave from the Institute of Physics and Nuclear Techniques, Academy of Mining and Metallurgy, Mickiewicza 30, 30-059 Kraków, Poland. For correspondence use this address.

of one hydrogen isotope and possible admixtures of elements with $Z > 1$ is depicted in Fig. 1. The muon creates an excited μ-atom [10] which cascades down to the ground state in several intermediate steps. A μ-molecule (ddμ or ttμ) is then formed, which possibly also undergoes deexcitation through one or more energy levels before fusion in it takes place. The fusion event ends one catalysis cycle. The muon which can be released in this process with probability $(1-\omega)$ reenters the chain to initiate another cycle. At any node of the chain the muon may decay or it can be irreversibly transferred to the element with $Z > 1$ as indicated in the figure.

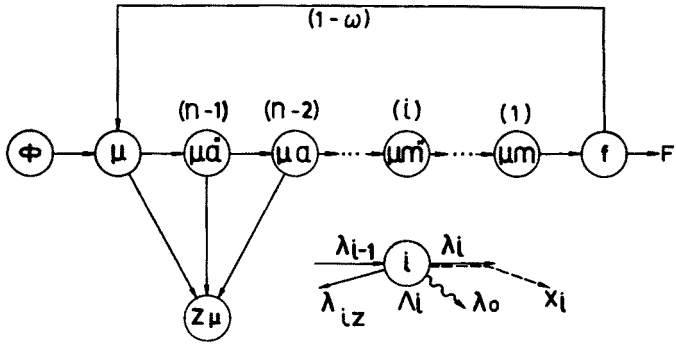

Fig. 1. Schematic graph presenting the muon-catalysis fusion chain in a target consisting of one hydrogen isotope (D_2 or T_2) and possible admixtures of elements with $Z > 1$

The transition rates between the nodes, λ_i, and the sticking coefficient, ω, which characterize the muon-catalyzed fusion chain can be most naturally determined from the time distributions of the fusion events ending the consecutive cycles and the analogous distributions of the signatures of other processes in the sequence. Such distributions are described by a set of particle-balance equations, one for each node, which are usually referred to as kinetic equations. Solutions of the kinetic equations have been discussed in different approximations by several authors, both for the mixtures of hydrogen isotopes [11–16] and, in more detail, for the one-component targets [17–20]. So far, attention has been focused mainly on the "all-cycles" (AC) solutions which describe sums of the considered quantities taken over all cycles initiated by a single muon. Recently, the kinetic formulae have been also obtained which describe the separate cycles of the muon-catalysis chain in one-component targets[1] [18–20]. Such a cycle-by-cycle description is better suited for experiments in which only a limited number of cycles is registered. In [18] it has been assumed that kinetics of the chain is determined solely by the process of μ-molecule formation. This is justified for the (d+d)μ-fusion where the rates of other processes are expected to be much higher ($\geqq 10^9$ s^{-1}) [5, 10] so that, at least for $t \gg 1$ ns, their influence on the time distributions can be neglected. In [19, 20] nuclear synthesis in the μ-molecule has been additionally taken into account to obtain the formulae relevant for the description of the (t+t)μ chain, where the corresponding fusion rate can be as low as 10^7 s^{-1} [21].

[1] In [20] an approximate cycle-by-cycle formula for the (d+t)μ-fusion is also presented.

In the present paper we derive cycle-by-cycle kinetic formulae which enable one to introduce any number of the intermediate steps leading to the muon catalyzed synthesis, i.e., besides the processes mentioned above, the creation of μ-atoms and μ-molecules in the excited states and their deexcitation towards the ground state. Although the rates of these processes are expected to be rather high ($\geqq 10^8$ s^{-1}) [5] and, so far the corresponding nodes have been usually replaced by single μ-atomic and μ-molecular vertices, we avoid this assumption and leave this question open for the experimental investigation.

By introducing appropriate admixtures of elements with $Z > 1$ information about the rates of processes in pure deuterium or pure tritium can be supplemented to include the rates of muon transitions from hydrogen isotopes to heavier nuclei. Transitions to helium are here of a primary importance both for the theoretical interest [5] and the fact that, since ^{4}He and ^{3}He are produced in the D_2–T_2 targets, helium can be expected to be the main fuel poisoning factor to be taken into account in planning a "cold fusion" power generator.

The analysis presented below concerns only the evolution in time of the muon-catalyzed fusion chain without taking into account any space dependence. Also, the concentration of fuel components is assumed to be constant over the time interval considered, which is a sufficient approximation in experiments on the muon-catalyzed fusion, although, it may not be true in an actual power generator. Moreover, no energy dependence of the transition rates is explicitly included, which has been a common assumption made so far in the literature; thus, the transition rates should be considered as appropriate averages.

2. *First cycle equations*

The kinetic equations describing the first cycle (no muon feedback) are:

$$\begin{aligned}
\frac{dN_f(t)}{dt} &= \lambda_1 N_1(t) \\
\frac{dN_1(t)}{dt} &= -\Lambda_1 N_1(t) + \lambda_2 N_2(t) \\
&\cdots\cdots\cdots\cdots\cdots\cdots \\
\frac{dN_i(t)}{dt} &= -\Lambda_i N_i(t) + \lambda_{i+1} N_{i+1}(t) \\
&\cdots\cdots\cdots\cdots\cdots\cdots \\
\frac{dN_n(t)}{dt} &= -\Lambda_n N_n(t) + \frac{d\Phi(t)}{dt},
\end{aligned} \tag{1}$$

where $N_i(t)$ are particle numbers in each of the nodes in Fig. 1, $\Phi(t)$ represents the muon source, and

$$\Lambda_i = \lambda_i + \lambda_0 + \sum_Z \lambda_{i,Z}, \tag{2}$$

where λ_i are transition rates between the nodes, $\lambda_0 = 0.455\ \mu s^{-1}$ is the muon decay rate and $\lambda_{i,Z}$ are the corresponding rates of transitions to heavier elements contaminating the target. Let us choose for the initial conditions: $N_i(0_-) = 0$ and $\Phi(0_-) = 0$. It should be noticed that $\lambda_{i,Z}$ are interaction rate constants proportional to target density, ϱ, and impurity concentration, c_Z: $\lambda_{i,Z} = \varrho c_Z \langle \sigma_{iZ} v_i \rangle$. Analogously, for the μ-atom and μ-molecule formation one has: $\lambda_i = \varrho(1-c_Z)\langle \sigma_{i,i-1} v_i \rangle$, the average of the corresponding cross section and relative velocity being taken over the Maxwell distribution at target temperature.

If an $i \to i-1$ transition has a detectable signature (e.g., a fusion-product α-particle or neutron or, at least in principle, an Auger-electron emitted in the nonresonant μ-molecule formation) then the time distribution of these signatures, $x_i(t)$, is determined by the number of particles in the i-th node, $N_i(t)$, and the corresponding transition rate λ_i:

$$x_i(t) = \frac{dX_i(t)}{dt} = \lambda_i N_i(t). \tag{3}$$

In particular, for the signatures of the fusion events we have:

$$F(t) = \frac{dN_f(t)}{dt} = \lambda_1 N_1(t) \tag{4}$$

and correspondingly for the time distribution of the $Z\mu$-atoms

$$\frac{dN_{Z_\mu}}{dt} = \sum \lambda_{i,Z} N_i(t), \tag{5}$$

where summation goes over the muonic and μ-atomic nodes.

After taking the Laplace transform of Eq. (1) one obtains:

$$N_f(s) = G_1^{(n)}(s)\Phi(s), \tag{6}$$

where

$$G_1^{(n)}(s) = \prod_{i=1}^{n} \frac{\lambda_i}{s+\Lambda_i}, \tag{7}$$

s denotes the Laplace transform parameter and n is the number of nodes in the chain. (The subsidiary nodes (Φ) and (f) are not counted).

3. *"All-cycles" (AC) solution*

The solution for all cycles is readily obtained from Eqs. (6)–(7) by closing the muon feedback loop:

$$N_f^{(AC)}(s) = G^{(n)}(s)\Phi(s), \tag{8}$$

where

$$G^{(n)}(s) = \frac{G_1^{(n)}(s)}{1-(1-\omega)G_1^{(n)}(s)}. \tag{9}$$

For $\Phi(t)$ given by the step function which corresponds to one muon entering the target at $t = 0$, the Laplace transform of the AC-time distribution of fusion events is:

$$F^{(AC)}(s) = G^{(n)}(s) = \frac{\prod_{i=1}^{n} \lambda_i}{\prod_{i=1}^{n} (s+\Lambda_i) - (1-\omega)\prod_{i=1}^{n} \lambda_i}. \tag{10}$$

The most immediate result following from Eq. (10) is the formula for the AC-yield of fusion events:

$$Y^{(AC)} = \int_0^\infty F^{(AC)}(t)dt = F^{(AC)}(s=0) = \frac{\prod_{i=1}^{n} \lambda_i}{\prod_{i=1}^{n} \Lambda_i - (1-\omega)\prod_{i=1}^{n} \lambda_i}. \tag{11}$$

The AC-time distribution of fusion events can be obtained by taking the inverse transform of (10):

$$F^{(AC)}(t) = \left(\prod_{i=1}^{n} \lambda_i\right) \sum_{i=1}^{n} \frac{e^{r_i t}}{\prod_{\substack{j=1 \\ j\neq i}}^{n} (r_i - r_j)}, \tag{12}$$

where r_i are zeros of the denominator in the RHS of Eq. (10). (Since $(1-\omega) < 1$ and $\Lambda_i > \lambda_i$ all r_i are negative.)

4. *Cycle-by-cycle kinetics*

The time distributions for the separate cycles are of great importance both for understanding of the kinetics of the muon-catalyzed fusion and for the analysis of the experimental data.

Let us expand $F^{(AC)}(s)$ in terms of $(1-\omega)$. From Eq. (9) one has

$$F^{(AC)}(s) = \sum_{k=1}^{\infty} (1-\omega)^{k-1}[G_1^{(n)}(s)]^k = \sum_{k=1}^{\infty} F_k(s). \tag{13}$$

In the time variable Eq. (13) reads:

$$F_k(t) = (1-\omega)^{k-1} \underbrace{F_1(t) * F_1(t) * \ldots * F_1(t)}_{(k\text{-}1)\text{fold convolution}}, \tag{14}$$

which, in an obvious interpretation [19], gives the time distribution of fusion events ending a k-th cycle.

In analogy to Eq. (11), the k-th cycle yield is then:

$$Y_k = (1-\omega)^{k-1}\left(\prod_{i=1}^{n}\frac{\lambda_i}{\Lambda_i}\right)^k. \tag{15}$$

Again, the k-th cycle time distribution of fusion events can be written as:

$$F_k(t) = (1-\omega)^{k-1}\left(\prod_{i=1}^{n}\lambda_i\right)^k Q_k^{(n)}(\Lambda_1, \ldots, \Lambda_n; t) \tag{16}$$

where

$$Q_k^{(n)}(\Lambda_1, \ldots, \Lambda_n; t) = \mathscr{L}^{-1}\left(\prod_{i=1}^{n}\frac{1}{s+\Lambda_i}\right)^k. \tag{17}$$

The inverse Laplace transform in Eq. (17) is:

$$Q_k^{(n)}(\Lambda_1, \ldots, \Lambda_n; t) = \frac{(-1)^{(n-1)k}}{[(k-1)!]^{n-1}}\sum_{j=1}^{k}\frac{t^{k-j}}{(j-1)!(k-j)!}$$

$$\times\sum_{i=1}^{n}e^{-\Lambda_i t}\sum_{\substack{l_1 \ldots l_p \ldots l_n \\ p\neq i}}\binom{j-1}{l_1 \ldots l_p \ldots l_n}\frac{(k-1+l_1)! \ldots (k-1+l_n)!}{\prod_{\substack{p=1 \\ p\neq i}}^{n}(\Lambda_i-\Lambda_p)^{k+l_p}}. \tag{18}$$

In the Appendix we list the explicit formulae for the first four nodes.

The yields and time distributions of the signatures associated with $(i) \to (i-1)$ transitions in the k-th cycle of the μ-catalysis chain can be found from the relation

$$x_i(s) = (1-\omega)^{k-2}[G_1^{(n)}(s)]^{k-1}(1-\omega)\prod_{j=n}^{i}\frac{\lambda_j}{s+\Lambda_j}, \tag{19}$$

which represents the convolution of $F_{k-1}(t)$ for the preceding $(k-1)$ cycles with the function describing the k-th cycle, truncated at the i-th node.

If there are more than one nuclear synthesis channels (as in the d+d fusion) the time distribution of their signatures can be obtained by substituting in Eqs. (15)–(19):

$$(1-\omega)\lambda_1 \to \sum_j (1-\omega_j)\lambda_{1,j} \tag{20}$$

with

$$\lambda_1 = \sum_j \lambda_{1,j} \tag{21}$$

and multiplying the resulting expression by the branching ratio $b_j = \lambda_{1,j}/\lambda_1$, $\lambda_{1,j}$ being the transition rate into the j-th channel and ω_j the corresponding sticking coefficient.

In most experiments the signatures of fusion and the internode transitions are detected with efficiency $\varepsilon < 1$. According to the arguments of Refs. [18, 19] the Laplace transform of the time distribution of the first registered cycle is:

$$\bar{F}_1(s) = \varepsilon \sum_{k=1}^{\infty} (1-\varepsilon)^{k-1} F_k(s), \tag{22}$$

which, using Eqs. (10, 13), can be written as:

$$\bar{F}_1(s) = \varepsilon \frac{\prod_{i=1}^{n} \lambda_i}{\prod_{i=1}^{n} (s+\Lambda_i) - (1-\omega)(1-\varepsilon) \prod_{i=1}^{n} \lambda_i}, \tag{23}$$

where ε is the experimental registration efficiency of fusion events. Analogously to Eq. (14) the corresponding expression for the k-th registered cycle is

$$\bar{F}_k(s) = (1-\omega)^{k-1} [\bar{F}_1(s)]^k. \tag{24}$$

Thus $\bar{F}_k(t)$ can be obtained by substituting in Eq. (16):

$$(\prod \lambda_i) \to \varepsilon \prod \lambda_i, \quad \Lambda_i \to -s_i, \tag{25}$$

where s_i are zeros of the denominator in Eq. (23). Analogously, for several fusion channels, substitutions (20) and (21) with $(1-\omega_j) \to (1-\omega_j)(1-\varepsilon_j)$ should be made and ε replaced in Eq. (23) by $\varepsilon_j b_j$, where ε_j is the registration efficiency for the j-th channel and b_j is the corresponding branching ratio.

5. *Discussion*

To illustrate the obtained dependences we show in Figs. 2–5 the time distributions of fusion events ending the first few cycles[2]. In all figures $\omega = 0.1$ which is approximately the value of the sticking coefficient in both $(d+d)\mu \to (^3He+n)\mu$ [8] and $(t+t)\mu \to (^4He+n)\mu$ [22].

Fig. 2 illustrates for a one-component target with the concentration of admixtures $c_Z = 0$ the effect of introducing the consecutive nodes with the internode transition rates differing by one order of magnitude: $\lambda_1 = 1\ \mu s^{-1}$, $\lambda_2 = 10\ \mu s^{-1}$, $\lambda_3 = 100\ \mu s^{-1}$ and $\lambda_4 = 1000\ \mu s^{-1}$. It is seen that the introduction of an additional node with λ by one order of magnitude larger than the previous one gives in this range of λ_i a significant effect even at quite large t, especially in the higher cycles. This effect is even more pronounced for $\varepsilon < 1$ (not shown in the figure) which is quite obvious as many cycles contribute

[2] The curves were obtained using the four-node formula (A.4) of the Appendix. Curves for fewer nodes (n = 1–3) were computed using also Eq. (A.4) and switching-off some of the nodes by putting the corresponding λ_i very large.

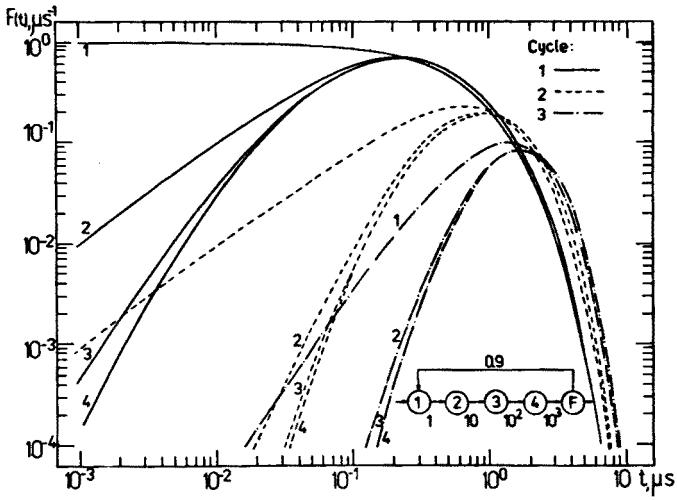

Fig. 2. Time distributions of the first three cycles initiated by a single muon at $t = 0$ for $\lambda_1 = 1\ \mu s^{-1}$, $\lambda_2 = 10\ \mu s^{-1}$, $\lambda_3 = 100\ \mu s^{-1}$ and $\lambda_4 = 1000\ \mu s^{-1}$. The number of nodes included in an increasing order is indicated at the curves. Registration efficiency is $\varepsilon = 1$ and no contaminations by $Z > 1$ are present

here to the first registered cycle. The apparent advantage of observing the contributions from the high-λ processes at large t in experiments with small ε is reduced, however, by the decrease in statistics. In planning the experiment the interplay of these two factors should be taken into consideration.

In Fig. 3 we illustrate the situation which may arise in experiments with pure liquid deuterium or pure liquid tritium targets ($c_Z = 0$). The curves in Fig. 3a are for the (d+d)μ--fusion in liquid deuterium where $\lambda_m \cong 0.1\ \mu s^{-1}$ (ddμ-formation [23]), $\lambda_f \cong 10^3\ \mu s^{-1}$ (fusion in ddμ) [24], $\lambda_{casc} \cong 5 \cdot 10^4\ \mu s^{-1}$ ($d\mu^* \to d\mu_0$ cascade to the ground state in dμ [25]) and $\lambda_a \cong 10^6\ \mu s^{-1}$ (dμ-atom formation [26]). Curves labeled by 1 and 2 correspond, respectively, to the 1-node (λ_m only) and the 2-node (λ_m, λ_f) solution. The contributions from λ_{casc} and λ_a become visible only below 1 ns.

According to the theoretical predictions, the rate of fusion in the ttμ-molecule may have values between 10 and $10^3\ \mu s^{-1}$, depending on the assumptions involved in the calculations [21] and, in liquid tritium, $\lambda_m \cong 3\ \mu s^{-1}$ [27]. Fig. 3b shows for the first three cycles the one-node time distributions together with the curves calculated with inclusion of different λ_f. It is seen that in the second cycle $\lambda_f = 100\ \mu s^{-1}$ gives a significant contribution even at $t \approx 100$ ns while the effect of $\lambda_{casc} = 5 \cdot 10^4\ \mu s^{-1}$ becomes visible only in the region of a few nanoseconds.

Figs. 4 and 5 present the effect of contaminating the liquid tritium target by adding the admixtures of heavier elements. In Fig. 4 the situation is shown in which only the muon transfer to impurities from the ground state is taken into account so that $\Lambda_2 = \lambda_m + \lambda_0 + \sum_Z \lambda_{t\mu,Z\mu}$. The last term is varied to account for different admixture concentration and composition. Curves A correspond to $c_Z = 0$ ($\Lambda_2 = \lambda_0 + \lambda_m = 3.5\ \mu s^{-1}$), curves B and C to contaminations giving $\sum \lambda_{t\mu,Z\mu}$ of the order of $\sim 10^1\ \mu s^{-1}$. (For $Z > 2$ the

transition rates $\lambda_{H\mu,Z\mu}$ are of the order of 10^5 s^{-1} [28] after reduction to $c_Z = 1$ and liquid hydrogen density). Λ_1 which is determined by λ_f is not affected by the admixtures. As expected, the large time tails become steeper and differ considerably for different hypotheses. The curves are determined practically by the first two nodes and the effect of including Λ_3 with λ_{casc} as in Fig. 3 becomes pronounced only below 10 ns.

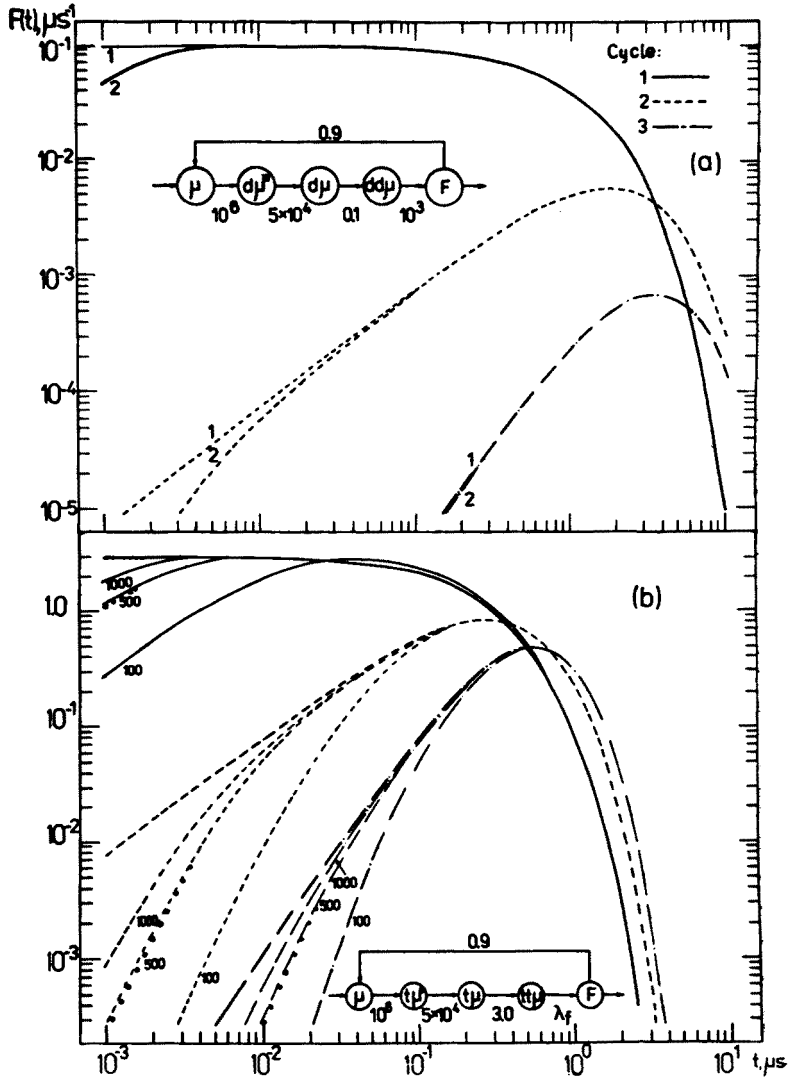

Fig. 3. Time distributions of the first three cycles initiated by a single muon at $t = 0$: a) for $\lambda_m = 0.1\ \mu s^{-1}$, $\lambda_f = 10^3\ \mu s^{-1}$, $\lambda_{casc} = 5 \cdot 10^4\ \mu s^{-1}$, $\lambda_a = 10^6\ \mu s^{-1}$ (as in case of (D+D)μ-fusion). (Contributions from λ_{casc} and λ_a become visible only below 1 ns); b) for $\lambda_m = 3\ \mu s^{-1}$, $\lambda_{casc} = 5 \cdot 10^4\ \mu s^{-1}$, $\lambda_a = 10^6\ \mu s^{-1}$ and varying λ_f ((T+T)μ-fusion). The values of λ_f are indicated at the curves. Thick lines are for 1-node solution (λ_m only), and the thin ones for 2-nodes (λ_f included). For $\lambda_f = 500\ \mu s^{-1}$ the effect of including λ_{casc} is indicated by the dots. Other comments as in Fig. 2

Let us remark that neglecting transitions to $Z\mu$ from the excited states was a common assumption in earlier studies of muon-catalyzed fusion. It was pointed out only recently [5] that such transitions might play an important role in the kinetics of this process. This is illustrated in Fig. 5a which shows analogous curves with Λ_2 fixed at 10.5 μs^{-1} and different hypothesis for $\Lambda_3 = \lambda_0 + \lambda_{casc} + \Sigma\lambda_{t\mu^*,Z}$ tried. Curves A correspond to the case considered in Fig. 4, curves B and C to a situation which may arise if transitions

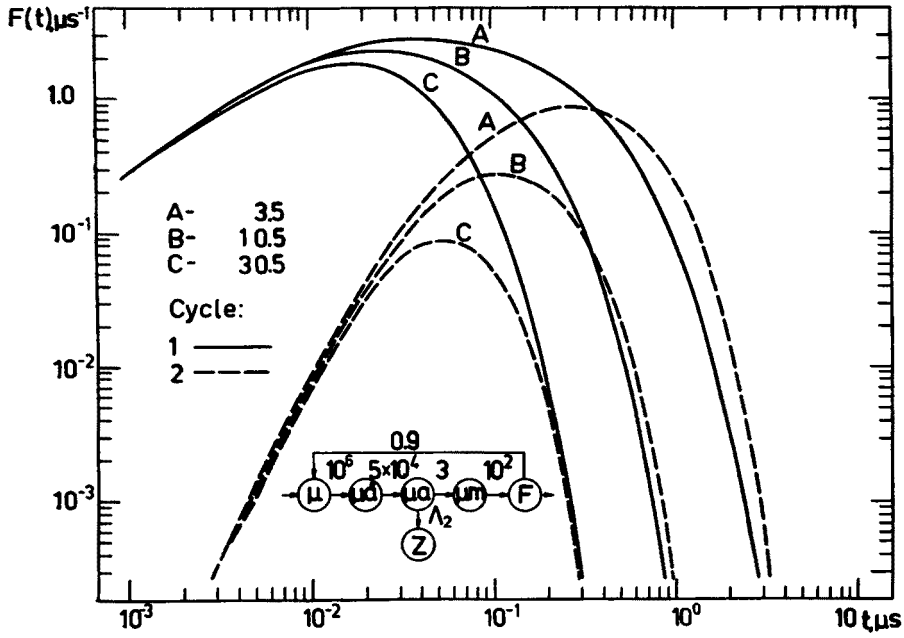

Fig. 4. Time distributions of the first two cycles for $\varepsilon = 1$, $\lambda_m = 3\ \mu s^{-1}$, $\lambda_f = 100\ \mu s^{-1}$, $\lambda_{casc} = 5 \cdot 10^4\ \mu s^{-1}$, $\lambda_a = 10^6\ \mu s^{-1}$. Λ_2 is varied as indicated in the figure, $\Lambda_i = \lambda_i + \lambda_0$ for $i \neq 2$

to Z from the excited states are significantly faster than from the ground state [5], so that they can compete with deexcitation of the μ-atoms ($\lambda_{casc} \approx 5 \cdot 10^4\ \mu s^{-1}$) even and low c_Z.

Direct capture of the muon by the $Z > 1$ impurities proceeds with a rate similar to muonic hydrogen formation [10]. Thus at small c_Z direct $Z\mu$ formation can be expected to have little influence on the distributions of the signatures in the chain. Fig. 5b illustrates a situation where the proportion of $H\mu$ to $Z\mu$ atoms directly formed is 5 : 1 with Λ_2 fixed at 30 μs^{-1}. For comparison, curves corresponding to the hypotheses described above for Λ_3 are also presented. For all curves in Fig. 5 : $\lambda_f = 100\ \mu s^{-1}$. As is seen in Figs. 5a and 5b presence of higher nodes is strongly reflected in the time distributions. However, in the region of $t \geqslant 10$ ns the effect is practically reduced to multiplication of the curve for $c_Z = 0$ by a factor λ_i/Λ_i which is obvious from Eqs. (16)–(18). More delicate effects appear only below 1 ns. Let us remark that the modification of Λ_i is determined by the product of the known heavy element concentration, c_Z, and an unknown exchange rate, $\lambda_{i,Z}$.

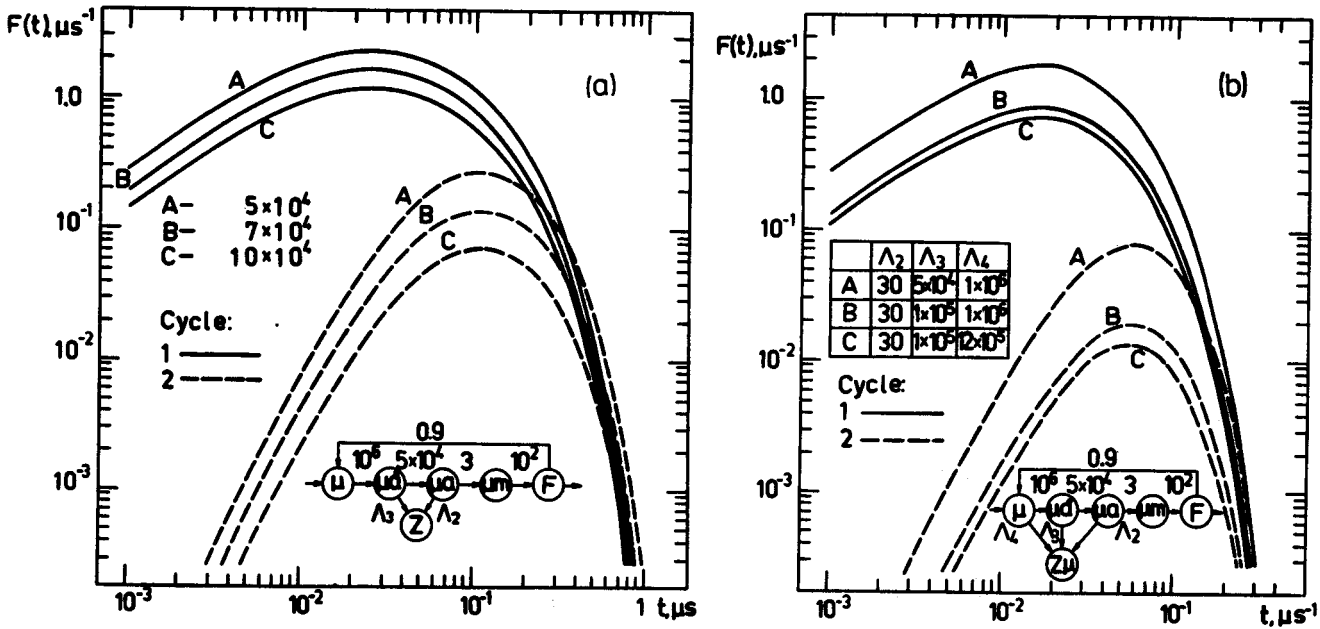

Fig. 5. Time distributions of the first and second cycle for $\varepsilon = 1$, $\lambda_f = 100\ \mu s^{-1}$, $\lambda_m = 3\ \mu s^{-1}$, $\lambda_{casc} = 5 \cdot 10^4\ \mu s^{-1}$, $\lambda_a = 10^6\ \mu s^{-1}$. a) Λ_2 is fixed at 10.5 μs^{-1} and Λ_3 is varied as indicated in the figure, b) Λ_2 is fixed (30 μs^{-1}), Λ_3 and Λ_4 are varied as indicated in the figure

6. *Conclusions*

The formulae presented above provide a practical tool for the interpretation of the experimental data on the muon-catalyzed fusion in D_2 or T_2 targets. Let us first remark that the time distributions (16)–(18) are invariant with respect to permutation of λ_i and independently of Λ_i, which is a generalization of the result of Refs. [17, 19]. Thus, assigning the experimental transition rates to the particular nodes will require the use of variation of λ_i and Λ_i with temperature (λ_m), target density[3] (λ_m, λ_a) or heavy element concentration c_Z (Λ_a, Λ_{casc}, Λ_m). In this respect measuring the signatures of other transitions in the chain could provide useful additional information.

As is seen from the discussion in the previous Section, even relatively high transition rates can be appreciated in the 10–100 ns region, especially in the high statistics measurements of the time distribution of the second or third cycle. Information from such experiments performed in pure deuterium and pure tritium can be a helpful input for the analysis of the muon-catalyzed fusion in deuterium-tritium mixtures.

The authors are indebted to Prof. L. I. Ponomarev for the stimulating discussions which have led to this investigation. They also thank their colleagues M. P. Faifman, V. S. Melezhik, L. I. Menshikov and J. Woźniak for helpful conversations. Two of the authors (M. B. and A. G.) thank Prof. V. P. Dzhelepov for his hospitality during their stay at JINR. One of them (M. B.) expresses his gratitude to Dr. E. P. Shabalin for creating conditions which enabled him to participate in this work.

APPENDIX

The explicit expressions for $Q_k^{(n)}(\Lambda_1, \ldots, \Lambda_n, t)$ according to Eq. (18) are:

$$Q_k^{(1)}(\Lambda_1, t) = \frac{t^{k-1}}{(k-1)!} e^{-\Lambda_1 t}, \tag{A.1}$$

$$Q_k^{(2)}(\Lambda_1, \Lambda_2, t) = \frac{(-1)^k}{(k-1)!} \sum_{j=1}^{k} \frac{(k+j-2)!}{(j-1)!\,(k-j)!} t^{k-j} \times \left[\frac{e^{-\Lambda_1 t}}{(\Lambda_1-\Lambda_2)^{k+j-1}} + \frac{e^{-\Lambda_2 t}}{(\Lambda_2-\Lambda_1)^{k+j-1}} \right], \tag{A.2}$$

$$Q_k^{(3)}(\Lambda_1, \Lambda_2, \Lambda_3, t) = \frac{1}{[(k-1)!]^2} \sum_{j=1}^{k} \frac{t^{k-j}}{(k-j)!} \sum_{l=0}^{j-1} \frac{(k+j-2-l)!\,(k-1+l)!}{l!(j-1-l)!} \times \left[\frac{e^{-\Lambda_1 t}}{(\Lambda_1-\Lambda_2)^{k+j-1-l}(\Lambda_1-\Lambda_3)^{k+l}} + \frac{e^{-\Lambda_2 t}}{(\Lambda_2-\Lambda_1)^{k+j-1-l}(\Lambda_2-\Lambda_3)^{k+l}} \right.$$

[3] This effect was discussed in detail for the 2-node AC-solution in Ref. [17].

$$+\frac{e^{-\Lambda_3 t}}{(\Lambda_3-\Lambda_1)^{k+j-1-l}(\Lambda_3-\Lambda_2)^{k+l}}\Bigg], \tag{A.3}$$

$$Q_k^{(4)}(\Lambda_1,\Lambda_2,\Lambda_3,\Lambda_4,t)=\frac{(-1)^k}{[(k-1)!]^3}\sum_{j=1}^{k}\frac{t^{k-j}}{(k-j)!}$$

$$\times\sum_{l=0}^{j-1}\sum_{m=0}^{j-1-l}\frac{(k-2+j-l-m)!(k-1+m)!(k-1+l)!}{l!\,m!(j-1-l-m)!}$$

$$\times\Bigg[\frac{e^{-\Lambda_1 t}}{(\Lambda_1-\Lambda_2)^{k+j-1-l-m}(\Lambda_1-\Lambda_3)^{k+m}(\Lambda_1-\Lambda_4)^{k+l}}$$

$$+\frac{e^{-\Lambda_2 t}}{(\Lambda_2-\Lambda_1)^{k+j-1-l-m}(\Lambda_2-\Lambda_3)^{k+m}(\Lambda_2-\Lambda_4)^{k+l}}$$

$$+\frac{e^{-\Lambda_3 t}}{(\Lambda_3-\Lambda_1)^{k+j-1-l-m}(\Lambda_3-\Lambda_2)^{k+m}(\Lambda_3-\Lambda_4)^{k+l}}$$

$$+\frac{e^{-\Lambda_4 t}}{(\Lambda_4-\Lambda_1)^{k+j-1-l-m}(\Lambda_4-\Lambda_2)^{k+m}(\Lambda_4-\Lambda_3)^{k+l}}\Bigg]. \tag{A.4}$$

In particular, for $n = 1$ and 2 our formulae coincide with the one- and two-node approximations of Refs. [18] and [19], respectively.

For the time distributions of the registered cycles (registration efficiency $\varepsilon < 1$) substitutions (25) have to be used. When several fusion channels are present the formulae should be modified as described in Section 4.

REFERENCES

[1] S. E. Jones et al., *Phys. Rev. Lett.* **51**, 1757 (1983); S. E. Jones et al., In Proceedings of the Third International Conference on Emerging Nuclear Systems, Helsinki, June 1983, published in *Atomkernenergie/Kerntechnik* **43**, 179 (1983).

[2] See the related papers in the Proceedings of the Third International Conference on Emerging Nuclear Systems, Helsinki, June 1983, *Atomkernenergie/Kerntechnik* vol. 43, No. 3 and 4, and in Contributions to the Muon-Catalyzed Fusion Workshop, Jackson-Hole, June 1984, Steven E. Jones Workshop Organizer, Idaho National Engeneering Laboratory, Idaho Falls, Idaho.

[3] F. C. Frank, *Nature* **160**, 525 (1947); A. D. Sakharov, Report Lebedev Inst. Acad. Sci. USSR, Moscow 1948; Ya. B. Zeldovich, *Dokl. Akad. Nauk SSSR* **95**, 494 (1954).

[4] M. Leon, *Phys. Rev. Lett.* **52**, 605 (1984); L. I. Menshikov, L. I. Ponomarev, *Pisma JETP* **39**, 542 (1984); S. E. Jones, Talk at Ninth International Conference on Atomic Physics, Seattle, July 1984.

[5] L. I. Ponomarev, Review talk at the Third International Conference on Emerging Nuclear Systems, Helsinki, June 1983, *Atomkernenergie/Kerntechnik* **43**, 175 (1983).

[6] J. Doede et al., *Phys. Rev.* **132**, 1782 (1963); J. Fetkovich et al., *Phys. Rev. Lett.* **4**, 570 (1960); P. Kammel et al., *Phys. Rev.* **A28**, 2611 (1983).

[7] V. M. Bystritsky et al., *Zh. Eksp. Teor. Fiz.* **76**, 460 (1979) (*Sov. Phys.-JETP* **49**, 232 (1979)).
[8] D. V. Balin et al., *Phys. Lett.* **141B**, 173 (1984).
[9] V. M. Bystritsky et al., *Pribory i Tekhnika Eksperimenta* **4**, 46 (1984); V. M. Bystritsky et al., Preprint JINR P13-84-59, Dubna 1984 (in Russian); V. M. Bystritsky et al., *Acta Phys. Pol.* **B15**, 689 (1984).
[10] For an extensive introduction into the subject see: S. S. Gershtein, L. I. Ponomarev, in: *Muon Physics*, Eds. V. M. Hughes and C. S. Wu, Academic Press, New York 1975, vol. III, p. 141; A. Bertin, A. Vitale, A. Placci, *Riv. Nuovo Cimento* **5**, 423 (1975); L. Bracci, G. Fiorentini, *Phys. Rep.* **86**, 169 (1982).
[11] S. S. Gershtein et al., *Zh. Eksp. Teor. Fiz.* **78**, 2099 (1980) (*Sov. Phys.-JETP* **51**, 1053 (1980)).
[12] L. N. Somov, Report JINR P4-81-852, Dubna 1981 (in Russian).
[13] H. Takahashi et al., *Atomkernenergie/Kerntechnik* **36**, 195 (1980).
[14] S. G. Lie, A. A. Harms, *Nucl. Sci. Eng.* **80**, 124 (1982).
[15] A. P. Sguigna, A. A. Harms, *Atomkernenergie/Kerntechnik* **43**, 191 (1983).
[16] A. Kumar, *Atomkernenergie/Kerntechnik* **43**, 203 (1983); P. Kammel et al., *Atomkernenergie/Kerntechnik* **43**, 195 (1983).
[17] V. M. Bystritsky et al., *Acta Phys. Pol.* **B15**, 699 (1984).
[18] V. G. Zinov, L. N. Somov, V. V. Filchenkov, Preprint JINR P15-82-478, Dubna 1982 (in Russian).
[19] V. M. Bystritsky, A. Guła, J. Woźniak, *Atomkernenergie/Kerntechnik* **45**, 197 (1984).
[20] V. G. Zinov, L. N. Somov, V. V. Filchenkov, Preprint JINR P4-84-45, Dubna 1984 (in Russian).
[21] V. S. Melezhik, Report JINR P4-81-463, Dubna 1981 (in Russian).
[22] S. S. Gerstein et al., *Zh. Eksp. Teor. Fiz.* **80**, 1690 (1981) (*Sov. Phys.-JETP* **53**, 872 (1981)); L. Bracci, G. Fiorentini, *Nucl. Phys.* **A364**, 383 (1981).
[23] Ya. B. Zeldovich, S. S. Gerstein, *Usp. Fiz. Nauk* **71**, 581 (1960); S. Cohen, D. L. Judd, R. J. Riddel, *Phys. Rev.* **119**, 384 (1960); L. I. Ponomarev, S. I. Vinitsky et al., *Zh. Eksp. Teor. Fiz.* **74**, 849 (1978). For the experimental values see Ref. [6].
[24] L. M. Bogdanova et al., *Phys. Lett.* **115B**, 171 (1982).
[25] M. Leon, H. Bethe, *Phys. Rev.* **127**, 636 (1962); V. E. Markushin, *Zh. Eksp. Teor. Fiz.* **80**, 35 (1981) (*Sov. Phys.-JETP* **53**, 17 (1981)); G. Ya. Korenman, *Yad. Fiz.* **32**, 916 (1980) (*Sov. J. Nucl. Phys.* **32**, 472 (1980)).
[26] J. S. Cohen, R. L. Martin, W. R. Wadt, *Phys. Rev.* **24A**, 33 (1981). (See also Ref. [24]).
[27] L. I. Ponomarev, M. P. Faifman, *Zh. Eksp. Teor. Fiz.* **71**, 1689 (1976) (*Sov. Phys.-JETP* **44**, 886 (1976)).
[28] A. Placci, E. Zavatini, A. Bertin, A. Vitale, *Nuovo Cimento* **64A**, 1053 (1969). (See also Ref. [10] for other data).